The Astrophysical Journal, 643:1239–1244, 2006 June 1

OXYGEN ABUNDANCE AND ENERGY DEPOSITION IN THE SLOW CORONAL WIND

E. Antonucci, L. Abbo, and D. Telloni
Istituto Nazionale di Astrofisica (INAF)–Osservatorio Astronomico di Torino, Strada Osservatorio 20, 10025 Pino Torinese, Italy;
antonucci@to.astro.it
Received 2005 October 11; accepted 2006 February 1

ABSTRACT

Observations of the extended corona obtained with the Ultraviolet Coronagraph Spectrometer (UVCS) on board *the Solar and Heliospheric Observatory* (*SOHO*) during the solar minimum years 1996 and 1997 have been analyzed to derive the oxygen abundance in the outer corona. A comparison of the absolute coronal abundance, measured in the coronal regions surrounding the quiescent solar minimum streamers, to the heliospheric values confirms that these regions are the dominant sources of the slow solar wind. However, the inferred coronal abundances are consistent with the heliospheric values only in case the ion velocity distribution is anisotropic and enhanced across the coronal magnetic field. Thus this analysis also leads to the conclusion that energy is deposited in the slow coronal wind at least up to 2.7 $R_\odot$ and that the efficiency of energy deposition is likely to be related to the local coronal magnetic topology.

Subject headings: solar wind — Sun: corona — Sun: UV radiation

1. INTRODUCTION

Comparison of solar and heliospheric elemental composition provides the means to identify the coronal sources of the heliospheric wind streams. The aim of this study is to compare the absolute oxygen abundance measured in the coronal wind to that detected in situ in slow wind streams to substantiate the finding that the slow wind is generated at the edges of the solar minimum polar coronal holes, close to the streamer boundary (Antonucci et al. 2005).

In the upper chromosphere abundances can be affected by an atom-ion separation process depending on the element first ionization potential (FIP). This process leads to an enrichment of low-FIP elements (<10 eV) in the slow and fast wind relative to the photosphere; the effect, however, is more enhanced in the slow wind (von Steiger et al. 2000). Oxygen is an element with high-FIP (13.6 eV), the same as hydrogen; thus, its wind abundance should remain close to photospheric values, and its differentiation in fast and slow wind streams is expected to be low if any. Yet the Solar Wind Ion Composition Spectrometer instrument on board *Ulysses* reveals a tendency to a systematic variation of the oxygen abundance between 5.3×10^{-4} (8.7) and 6.3×10^{-4} (8.8), as the wind speed varies between 400 and 800 km s^{-1} typical values of the slow and fast wind streams, respectively (von Steiger et al. 1995). Hence, the heliospheric fast wind substantially retains the photospheric oxygen abundance, 6.7×10^{-4} (8.83), as determined by Grevesse & Sauval (1998), while the slow wind tends to be characterized by a lower abundance than the fast wind. However, according to a recent reassessment by Asplund et al. (2004), the photospheric abundance is found to be unexpectedly lower, 4.6×10^{-4} (8.66), than that measured both in the fast and slow wind streams; but this discrepancy might not be real due to possible systematic errors.

The emission of oxygen ions and hydrogen atoms is well observed in the outer solar corona, where H I Lyα λ1216 and the O VI $\lambda\lambda$1032 and 1037 are the most intense spectroscopic lines. Since plasma density becomes extremely low in the outer corona, these lines are dominantly formed by radiative resonance scattering. This fact has allowed us to identify the solar wind in the corona by deriving its expansion velocity via Doppler dimming, with the UVCS on board *SOHO* (e.g., Kohl et al. 1997).

Slow plasma outflows at a speed of 90 km s^{-1} are observed at the far edge of polar coronal holes, all along the streamer boundary (Antonucci et al. 2005) as well as above the streamer cusp, approximately beyond 3 $R_\odot$ (Abbo & Antonucci 2002; Strachan et al. 2002; Antonucci et al. 2005). It is plausible that a component of the slow wind is also originating inside streamers, as suggested in some studies stimulated by the finding of a depletion of oxygen in the core of quiescent solar minimum streamers. The oxygen emission shows a strong depletion in the streamer core combined with a moderate depletion in the bright regions surrounding the dim core (Noci et al. 1997; Raymond et al. 1997b; Marocchi et al. 2001). If a streamer consists of multiple regions of closed magnetic fields, open field lines channeling slow wind could well exist inside the streamer itself, and a smaller ion drag along these lines might explain the core abundance depletion (Noci et al. 1997). According to an alternative suggestion, slow winds might on the contrary arise from the streamer bright regions that in this case are identified with the streamer stalks (Raymond et al. 1997a). However, only upper limits on coronal expansion speed have been derived so far inside streamers (Frazin et al. 2003). The determination of oxygen abundance of the plasma flowing outside the streamer boundary is thus a key element to identify the dominant coronal source of the slow wind streams in the heliosphere.

2. OBSERVATIONS AND DIAGNOSTIC METHOD

The ultraviolet emission of the equatorial streamer belt was systematically observed with the *SOHO* UVCS (Kohl et al. 1997) in the solar minimum years 1996–1997. The aim of this study is to measure the absolute oxygen abundance in the coronal regions affected by low-speed expansion, which are observed outside coronal streamers at least above 1.8 $R_\odot$ (Antonucci et al. 2005, hereafter Paper I). The same data analyzed in Paper I are the object of this investigation. They consist of six streamers observed at high spectral resolution with UVCS, on 1996 August 19, 22, 30, and September 1, and on 1997 April 30 and May 5.

The intensities of the O VI $\lambda\lambda$1032 and 1037 and H I λ1216 lines are derived according to the procedures described in Paper I. Line intensities are averaged (1) over narrow lanes, 15°–20° wide, outside the streamer boundaries and (2) inside streamers,

in a region delimited by the boundaries. The interface between streamer and coronal hole is defined as the contour where the streamer peak emission decreases by $1/e$. The electron densities and outflow velocities of the slow wind, averaged over the data sample, are given in Paper I.

The absolute oxygen abundance N_O/N_H is derived from the ratio $I_{r,\,O\,VI}/I_{r,\,H\,I}$ of the radiative components of the O VI λ1032 and the H I λ1216 line intensities. The diagnostics adopted to infer the abundance takes into account both the coronal plasma expansion and the width of the absorbing profile of the coronal ions/atoms. In the outer corona, the radial component of the outflows induces Doppler dimming of the radiative component of line intensities. Doppler dimming also depends on the coronal absorbing profile, which can be very broad in the outer corona due to enhanced ion velocity distributions along the line of sight (e.g., Antonucci et al. 1997; Kohl et al. 1997).

The coronal H I λ1216 emission is predominantly radiative. The radiative component of the O VI λ1032 line, which is significantly excited by both radiation and collisions, can be isolated by using the intensities of the O VI doublet (Antonucci et al. 2004). The observed intensities of the O VI $\lambda\lambda$1032 and 1037 lines are given by the sums of their radiative and collisional components. The ratio R_1 of the radiative components of the two lines depends on atomic parameters and the plasma expansion velocity. The ratio R_2 of the collisional components of the two lines is related to atomic parameters only; it is a function of the electron temperature of the plasma being dependent on the ratio of the collisional excitation rate coefficients of the atomic transitions. Radiative and collisional components of the O VI doublet can then be derived since their are related by four equations, and in an expanding plasma they are derived as functions of the outflow velocity. In particular the ratio of the radiative components R_1 is given by

$$R_1 = \frac{I_{r,\,O\,VI\,\lambda1032}}{I_{r,\,O\,VI\,\lambda1037}} = \frac{(bB_{12}\lambda_0)_{1032}}{(bB_{12}\lambda_0)_{1037}} \frac{\int_{los}\int_\Omega \Phi(\delta\lambda_{1032})p(\varphi)\,d\omega n_i\,dl}{\int_{los}\int_\Omega \Phi(\delta\lambda_{1037})p(\varphi)\,d\omega n_i\,dl}, \tag{1}$$

$$R_1 \sim \frac{(bB_{12}\lambda_0)_{1032}}{(bB_{12}\lambda_0)_{1037}} \frac{\langle\int_\Omega \Phi(\delta\lambda_{1032})p(\varphi)\,d\omega\rangle}{\langle\int_\Omega \Phi(\delta\lambda_{1037})p(\varphi)\,d\omega\rangle}. \tag{2}$$

In equation (1) the quantity b is the branching ratio for radiative de-excitation, B_{12} is the Einstein coefficient for absorption, and λ_0 is the transition wavelength. The inner integral describes resonant scattering of the incident photons received in an infinitesimal solid angle $d\omega$ and accounts for Doppler dimming of line intensity due to the outflow velocity of the coronal plasma. The quantity $p(\varphi)$ takes into account the geometry of the scattering process. Resonant scattering, proportional to the ion density n_i, is then integrated along the line of sight (los). The dependence on the ion density and the integration along the los can be neglected when using the average along the los of the scattering process, $\langle\int_\Omega \Phi(\delta\lambda)p(\varphi)\,d\omega\rangle$ (eq. [2]).

The ratio R_1 then depends on the Doppler dimming factor introduced by the dynamics of the expanding plasma $\Phi(\delta\lambda)$:

$$\Phi(\delta\lambda) = \int_0^{+\infty} I_{ex}(\lambda - \delta\lambda, \boldsymbol{n})\Psi(\lambda - \lambda_0)\,d\lambda, \tag{3}$$

defined as the integral of the product of the intensity $I_{ex}(\lambda, \boldsymbol{n})$ of the exciting spectrum and $\Psi(\lambda)$ as the normalized coronal absorption profile along the direction of the incident radiation $\boldsymbol{n}$; $\delta\lambda$ is the shift of the disk spectrum introduced by the radial expansion velocity, $\boldsymbol{w}$, of the coronal absorbing ions/atoms along the direction $\boldsymbol{n}$:

$$\delta\lambda = \frac{\lambda_0}{c}\,\boldsymbol{w}\cdot\boldsymbol{n}. \tag{4}$$

The oxygen abundance is then given by the following equation:

$$\left(\frac{N_O}{N_H}\right) \sim \frac{I_{r,\,O\,VI}}{I_{r,\,H\,I}} \frac{b_{H\,I}}{b_{O\,VI}} \frac{B_{12,\,H\,I}}{B_{12,\,O\,VI}} \frac{\lambda_{0,\,H\,I}}{\lambda_{0,\,O\,VI}} \frac{n_{H\,I}/n_H}{n_{O\,VI}/n_O} \times \frac{\langle\int_\Omega \Phi(\delta\lambda_{H\,I})p(\varphi)\,d\omega\rangle}{\langle\int_\Omega \Phi(\delta\lambda_{O\,VI})p(\varphi)\,d\omega\rangle}. \tag{5}$$

The quantity $[(n_{H\,I}/n_H)/(n_{O\,VI}/n_O)](T_e)$ is the ratio of the concentrations of H I atoms and O VI ions, as a function of the electron temperature T_e. The intensity of the exciting spectrum has been measured on disk by Curdt et al. (2001).

Systematic uncertainties in deriving the oxygen abundance in a plasma that is either static or affected by negligible outflows, such as that confined in a streamer, are discussed in detail by Marocchi et al. (2001). In order to asses the effect of the dimming factors on the expected uncertainties of the inferred oxygen abundance in the slow coronal wind, in the approximation of equation (2) without performing a full integration along the los, we have used the following approach. The expected intensities of the O VI doublet and the H I Lyα line are computed on the basis of the electron density and outflow velocity derived in Paper I, for an electron temperature typical of coronal holes, and of the kinetic temperatures derived from the observed oxygen and hydrogen lines. The oxygen abundance of the slow heliospheric wind is assumed. The computation is performed by integrating the emission along the los in the approximation of cylindrical symmetry of the streamer belt. The line intensities so inferred are then analyzed in order to obtain the oxygen abundance via the approximated method discussed above, in the assumption of isotropic velocity distribution for the oxygen ions and the neutral hydrogen atoms. The derived abundances are underestimated by about 20% below 2 $R_\odot$ and less than 10% above that height.

The absolute oxygen abundance can be derived with equation (1) when the following conditions are fulfilled: (1) oxygen ionization equilibrium and (2) hydrogen ionization equilibrium. Otherwise equation (1) can be still used provided that appropriate approximations are taken into account. In the analysis the same expansion speed $\boldsymbol{w}$ for oxygen and hydrogen outflow components is assumed since in the slow coronal wind, according to the analyses performed up to now, there is no evidence for differences in outflows of the oxygen and hydrogen components. In what follows we check for the validity of this condition anyway.

3. CORONAL SLOW WIND TIMESCALES

The O VI ionization equilibrium timescale,

$$\tau_{eq}(O\ VI, r) = \frac{1}{\{c_j[T_e(r)] + a_j[T_e(r)] + \rho_i[T_e(r)] + d_i[T_e(r)]\}n_e(r)}, \tag{6}$$

is calculated by using the rates of collisional ionization c_j (Vornov 1997), autoionization a_j (Arnaud & Rothenflug 1985), radiative recombination ρ_i (Verner & Ferland 1996), and dielectronic

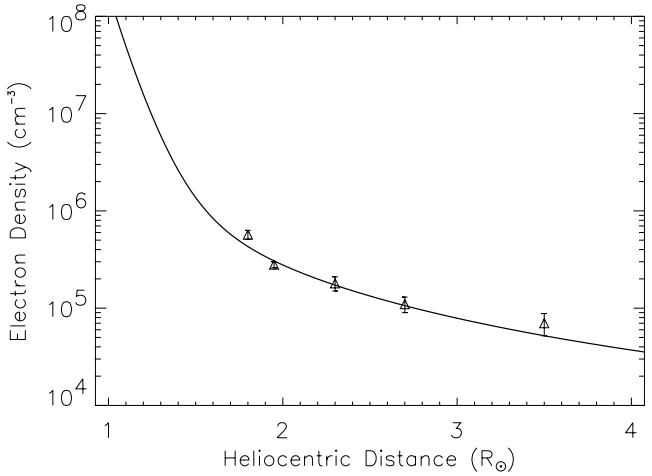

FIG. 1.—Electron density of the slow coronal wind flowing along the streamer boundaries; the experimental values derived by Antonucci et al. (2005) are shown as triangles.

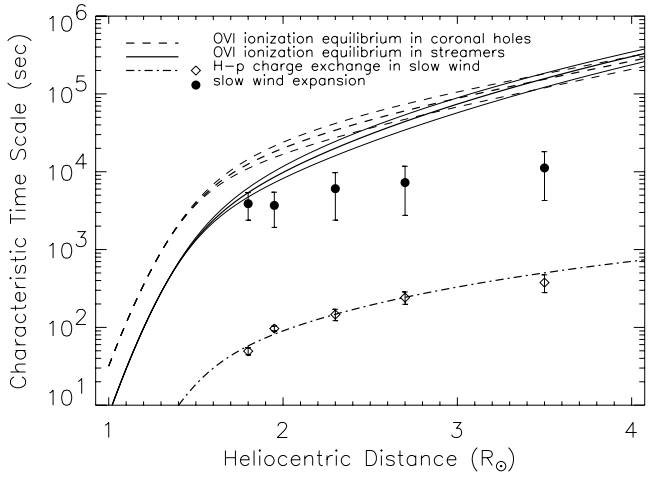

FIG. 2.—Plasma timescales in the slow coronal wind observed outside the streamer boundary for (1) O VI ionization equilibrium (the dashed line is computed with coronal hole electron temperature extrapolated from David et al. [1998] values, and the solid line is computed with streamer temperature as derived by Gibson et al. [1999]); (2) hydrogen-proton charge exchange (*diamonds fitted by a dot-dashed curve*); and (3) coronal expansion (*circles*).

recombination d_i (Mazzotta et al. 1998). The electron density curve, as a function of heliodistance r (Fig. 1),

$$n_e(r) = \left(\frac{1736.9}{r^{13.72}} + \frac{A}{r^B} + \frac{4.6}{r^2}\right) \times 10^5 \text{ cm}^{-3}, \quad (7)$$

fits the results obtained for the slow wind plasma in Paper I, with $A = 27.3$ and $B = 4.2$. The first term ensures that the fit tends to the density values of Guhathakurta et al. (1999) for low r; the last term ensures that electron density tends to the asymptotic interplanetary value. In the analysis of the slow wind performed in Paper I we have assumed that the regions surrounding the streamer boundaries are characterized by an electron temperature close to the coronal hole one. This parameter is not crucial in deriving the plasma outflow velocity in any case. This is not the case in deriving the plasma timescales and the oxygen abundance; therefore, in what follows we use two plausible limits for the electron temperature of the slow wind outside streamers: (1) the values extrapolated from the measurements by David et al. (1998), valid for the core of a coronal hole (see Antonucci et al. 2000), and (2) the Gibson et al. (1999) model, valid for streamers. The results for ionization equilibrium of oxygen five time ionized $\tau_{\rm eq}(\text{O VI}, r)$ obtained in the two limiting cases are plotted in Figure 2 (*dashed and solid lines*, for solar minimum coronal holes and streamers, respectively).

The timescales for oxygen ionization equilibrium are compared with the expansion time of the slow wind (e.g., Withbroe et al. 1982),

$$\tau_{\rm exp}(r) = \left(\frac{w}{n_e}\frac{dn_e}{dr}\right)^{-1} \quad (8)$$

(*circles*), in Figure 2. If the slow wind temperature approaches the streamer one, expansion (*circles*) occurs more rapidly than ionization beyond 1.8 $R_\odot$. Hence, in this case, the oxygen ion concentration $n_{\rm O\,VI}/n_{\rm O}(T_e)$ attained at about 1.8 $R_\odot$ for $T_e = 1.3 \times 10^6$ K remains frozen in the expanding plasma. If instead the slow wind temperature is closer to that found in the core of coronal holes, oxygen ionization freezes lower down, at about 1.6 $R_\odot$ (by extrapolation of the expansion time to lower altitudes). In the latter case, however, thermal conditions vary very slowly in the outer corona; hence, independent of the fact that the expansion time is shorter than that for ionization equilibrium, the ion concentration remains approximately constant.

The ionization equilibrium time for hydrogen, which is close to the characteristic time for charge exchange between hydrogen atoms and protons (Fig. 2, *dash-dotted line*), is attained in a time shorter than the expansion time out to 3.5 $R_\odot$. Hence, in the region of interest neutral hydrogen concentration $n_{\rm H\,I}/n_{\rm H}$ is always controlled by the local electron temperature. Thus since oxygen ionization equilibrium is not strictly verified in the expanding outer corona, equation (1) used to derive oxygen abundance can be still applied provided that (1) the oxygen ionization is frozen at $T_e = 1.3 \times 10^6$ K, in one limiting case (while the hydrogen ionization varies as a function of the Gibson et al. [1999] temperature) and (2) oxygen and hydrogen concentrations are both computed for a temperature close to that of coronal holes, in the other limiting case.

In the slow wind at least out to 4 $R_\odot$, protons and neutral hydrogen remain coupled, since charge exchange between hydrogen atoms and protons can be established in a time shorter than the expansion time (Fig. 2). In order to compute conditions of collisional equilibrium of O VI ions and protons (Fig. 3), determined by using the formulae by Spitzer (1962), oxygen abundance is set equal to 5.3×10^4 (von Steiger et al. 1995), a value valid for the slow wind. The ratio between proton and electron density is set equal to 0.83 for a fully ionized plasma with 10% helium. When computing collisional equilibrium of the two species, because of the uncertainty in the oxygen temperature, we assume the observed oxygen and hydrogen kinetic temperatures as limiting values for this quantity. In both cases the proton temperature can be set equal to the hydrogen temperature. The kinetic temperature measures the width of the velocity distribution of particles along the los, $T_k = (v_{1/e}^2 m_p A)/2k_{\rm B}$, where $v_{1/e}$ measures the broadening of the los velocity distribution of the atoms/ions, $k_{\rm B}$ is the Boltzmann constant, m_p is the proton mass, and A is the atom/ion mass number (and not necessarily measures the particle thermal conditions). According to the values T_k derived for the slow wind plasma in Paper I, the O VI temperatures can be up to 1 order of magnitude higher than the hydrogen one; for instance, at 3.5 $R_\odot$ we find values of 4×10^7 and 2×10^6 K, for oxygen and hydrogen, respectively. This is a reason to suggest that the ion

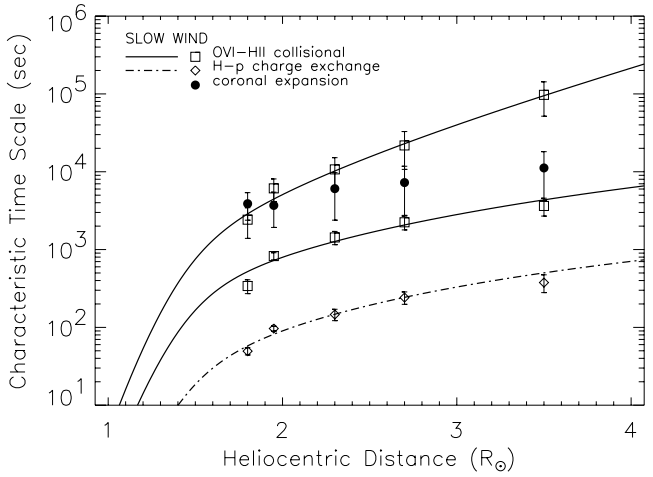

FIG. 3.—O VI and H II collisional equilibrium (*solid lines*) compared with expansion (*circles*) and the hydrogen-proton charge exchange (*diamonds*) timescales in the regions of acceleration of the slow wind outside the streamer boundary.

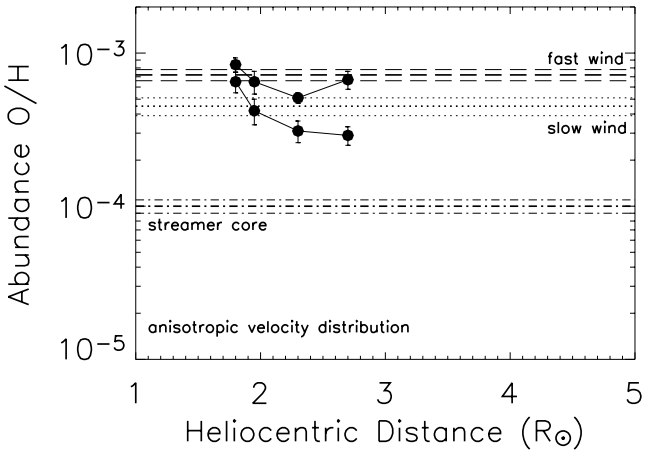

FIG. 4.—Oxygen abundance in the regions of slow expansion outside streamers, obtained for anisotropic velocity distribution of the oxygen ions. The upper and lower curves are obtained for the limits chosen for the slow wind temperature: upper limit (streamer temperature) and lower limit (coronal hole temperature), respectively.

velocity distribution is anisotropic, as in the case of the fast wind in the core of coronal holes, where extremely large velocity distribution are observed along the los (see Paper I). The collisional equilibrium timescale can then be considered delimited by two curves in Figure 3 (*solid lines*), where the upper one corresponds to ion temperature equal to kinetic temperature, and the lower one corresponds to ion temperature equal to hydrogen temperature. Figure 3 shows that almost out to 2.7 $R_\odot$ the slow wind expansion time is not significantly shorter than the upper limit for the collisional time; therefore, in this region oxygen ion and proton populations are substantially in equilibrium. Farther out, collisional equilibrium would be maintained only if oxygen and proton/hydrogen temperatures were equal. This means that at least up to about 2.7 $R_\odot$, the values of O VI and proton collisional timescales, combined with the fact that hydrogen and protons are still coupled, ensure that oxygen and hydrogen are flowing outward substantially at the same speed $\boldsymbol{w}$. This implies that Doppler shifts $\delta\lambda = (\lambda_0/c)\boldsymbol{w} \cdot \boldsymbol{n}$ in equation (1) are the same for oxygen and hydrogen.

4. ANALYSIS RESULTS

Due to the limitations imposed by the observational data available, it is possible to derive the oxygen abundance in the slow coronal wind flowing around streamers only in a relatively wide acceptance region. This is defined by assuming different velocity distributions of the O VI ions and for the two limiting electron temperatures used in the analysis. The abundance results averaged over the observation sample are plotted in Figures 4 and 5, in the hypothesis of anisotropic and isotropic ion velocity distribution, respectively. For the anisotropic case (Fig. 4) the ion temperature in the direction perpendicular to the los is set equal to the proton temperature, while along the los it coincides with the observed kinetic temperature. In the case of isotropy, T_k describes the width of the three-dimensional Maxwellian ion distribution (Fig. 5). In each figure, the upper and lower curves are derived by assuming the electron temperature equal to that found in streamers and coronal holes, respectively. Thus the region within the two curves defines the uncertainty of the oxygen abundance due to the fact that in the slow wind region temperature is not yet directly measured. The abundance is compared with that of the fast and slow heliospheric winds (*dashed and dotted lines*, respectively) and of the streamer core (as derived by Marocchi et al. [2001], *dash-dotted line*), where oxygen is highly depleted. The errors of the fast and slow wind abundance are derived by averaging the results obtained by von Steiger et al. (1995) for wind speed between 800 and 880 and 370–450 km s^{-1}, respectively.

The abundance results are clearly dependent on both the electron temperature and the anisotropy degree of the velocity distribution of oxygen ions in the slowly expanding coronal plasma. We find that the oxygen concentration of the slow coronal wind is consistent, within the statistical errors, with the heliospheric values of the low-speed wind streams provided that (1) the electron temperature is intermediate between the limits used in the analysis and (2) the oxygen ion velocity distribution is highly anisotropic (Fig. 4). It is interesting to note that lower down in the atmosphere, at 1.8 $R_\odot$, the oxygen coronal abundance is close to that of the fast wind. It then decreases with heliodistance to reach the slow wind conditions beyond about 2 $R_\odot$. If instead an isotropic velocity distribution is assumed, the values falling in the acceptance region, delimited by the curves derived for the extreme coronal electron temperatures (Fig. 5, *circles*), are

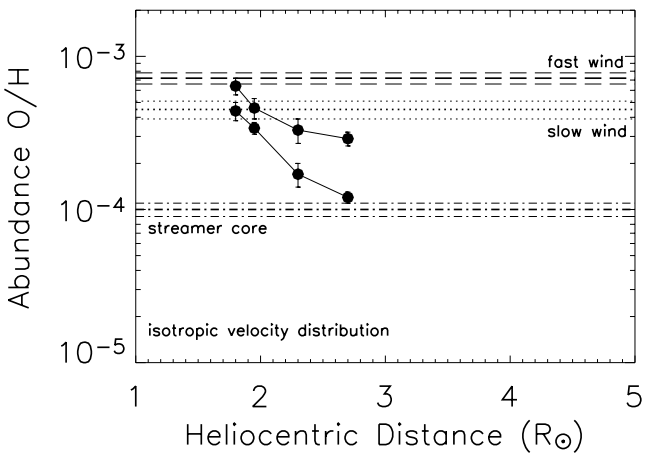

FIG. 5.—Oxygen abundance in the regions of slow expansion outside streamers, obtained for isotropic velocity distribution of the oxygen ions. The upper and lower curves are obtained for the limits chosen for the slow wind temperature: upper limit (streamer temperature) and lower limit (coronal hole temperature), respectively.

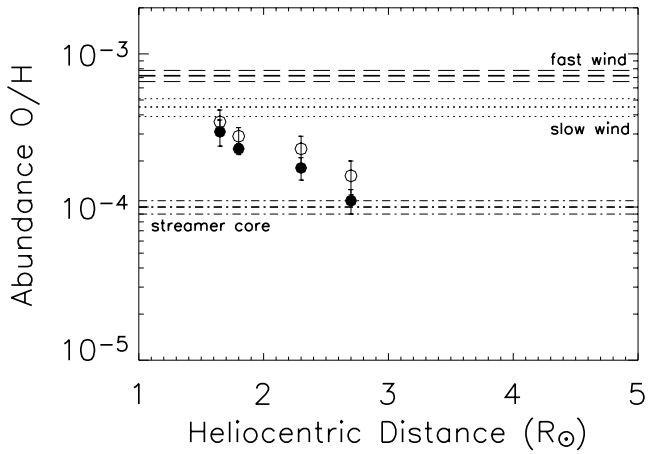

FIG. 6.—Average oxygen abundance in streamers. Filled circles refer to anisotropic ion velocity distribution, and open circles refer to the case of isotropy.

decreasing with height, and beyond 2 $R_\odot$ they become too low to be consistent with heliospheric composition. Furthermore, cooler electron temperatures, such as those of coronal holes (Fig. 5, *lower curve*), yield an abundance value decreasing at a higher rate with height, which reaches at 2.7 $R_\odot$ the composition found in the core of streamers.

We also derive the average oxygen abundance of the streamer plasma confined inside the boundaries, for comparison with the slow coronal wind composition (Fig. 6; filled circles indicate the results for anisotropic ion velocity distribution, and open circles refer to the isotropic case). The results are obtained by adopting the streamer density derived in Paper I and the electron temperature derived by Gibson et al. (1999). When averaging over the streamer region delimited by the boundaries, even if there the plasma is not fully confined, static conditions are dominant. Therefore the ion velocity distribution is expected to be isotropic, and the values obtained in this case best represent the average oxygen abundance in solar minimum quiescent streamers. Oxygen abundance inside streamers is increasingly lower than the slow wind value, and at 2.7 $R_\odot$ oxygen is depleted as in the streamer core.

5. DISCUSSION

The coronal plasma flowing at low speed, 90 km s^{-1}, along the boundaries of a solar minimum streamer is characterized by an oxygen abundance consistent, under plausible conditions, with the slow wind composition observed in the heliosphere. This consistency is found by applying the following constraints: (1) a temperature in between that of coronal hole and streamers and (2) an anisotropic ion velocity distribution (Fig. 4). On the contrary, inside streamers the average oxygen abundance rapidly falls with altitude, thus significantly diverging from the slow wind composition (Fig. 6). This rapid decrease with heliodistance is in agreement with previous streamer analyses (e.g., Marocchi et al. 2001) and implies that a streamer cannot be a substantial source of slow wind. Therefore these findings substantiate the conclusion that the narrow regions in the immediate proximity of streamers are the dominant coronal sources of the slow wind during solar minimum.

On the basis of the position of the lanes where the slow coronal wind flows, externally to the streamer boundaries, and of the fact that there the electron density is diverging from the fast wind value only above 1.8 $R_\odot$, it was suggested, in Paper I, that fast and slow winds have a common origin in coronal holes. That is, they share similar properties in the inner corona, but they differentiate during propagation in the outer corona. This differentiation predominantly occurs at the edges of a hole, where the flow tubes are characterized by much larger expansion factors due to the local magnetic topology. The present analysis supports this interpretation, since also the conditions of the oxygen abundance of the slow wind around 1.8 $R_\odot$ (Fig. 4) are very close to those found for the coronal and heliospheric fast wind [6.0×10^{-4} (8.78), Antonucci & Giordano 2001; 6.3×10^{-4} (8.8), von Steiger et al. 1995]. The heliospheric slow wind value is reached only farther out at a height of about 2 $R_\odot$. Therefore we conclude that core and edges of polar coronal holes, which show substantially the same physical properties at the base of the hole, do indeed change during the propagation along magnetic field lines of different divergence. Thus magnetic topology can be suggested as an important factor in determining the physical conditions of the expanding plasma in the outer corona, where solar wind approaches the heliospheric regime. In particular, the large expansion factors at the edges of coronal holes are intrinsically related to the formation of the slow wind conditions, as suggested on the basis of other considerations by Wang & Sheeley (1990).

When the wind plasma is rising from the solar surface, ion abundances can be modified by different processes, such as the process leading to the FIP effect presumably at the chromospheric level, Coulomb drag by part of protons, and gravitational settling in the corona. On the other hand, when the coronal wind expands into the heliosphere, its composition is substantially retained. On this basis, the consistency of coronal and heliospheric oxygen abundance was imposed in the present analysis. That is, consistency was ensured by satisfying the following constraints on the plasma properties in the region where the slow wind is accelerated: electron temperature has to be intermediate between coronal hole, and streamer temperature and oxygen ion velocity distribution has to be anisotropic, with enhanced broadening along the los. This conclusion has important consequences, since the inferred anisotropy can be interpreted as a signature of energy deposition in analogy with the interpretation of similar observations obtained in the core of coronal holes. In the fast coronal wind, above 1.8 $R_\odot$ the observed ratios of the Doppler dimmed O VI $\lambda\lambda$1032, 1037 intensities are indeed found to be consistent with a coronal model only when this is characterized by high anisotropy of the oxygen velocity distribution with enhanced broadening along the los. Hence the oxygen kinetic temperature observed in the coronal fast wind, which, however, is 1 order of magnitude higher than in the slow wind (see Paper I), has been ascribed to a preferential acceleration of ions along the los. Being the los roughly perpendicular to the simplified coronal magnetic field existing during solar minimum, it follows that oxygen ions are preferentially accelerated across the field, thus indicating an energy deposition process in the fast wind acting in that direction (e.g., Cranmer et al. 1999). In analogy with the fast wind case, we obtain information on energy deposition that occurs preferentially across the field also in the slow wind, although in this case the lower kinetic temperatures observed indicate that the process is less effective than in the fast wind. The above discussion leads then to the conclusion that the same heating process acting in the fast wind emerging from the core of holes, also occurs in the slow wind flowing at the edges of a polar coronal hole. The process, however, is less efficient, since in the slow wind the oxygen kinetic temperature, signature of preferential acceleration across the magnetic field, remains approximately 1 order of magnitude lower at 2.0–2.7 $R_\odot$ than in the core of coronal holes (Paper I; Fig. 3). The abundance results thus

confirm the suggestion put forward in Paper I that energy deposition is occurring from the core to the edges of a coronal hole according to the same process, but with a different efficiency. This difference is very likely related to the local magnetic topology, which significantly changes in the regions far from the core of the hole, when approaching the streamer boundary. As far as the mechanism for energy deposition is concerned, we expect that the same process invoked for accelerating the fast wind, which has been suggested to be wave dissipation via ion cyclotron resonance (Cranmer et al. 1999), is acting in the slow wind. The discussion on the oxygen abundance of the plasma expanding at slow speed in proximity of streamers then leads to the conclusion that energy is deposited not only in the fast but also in the slow coronal wind at the level of the outer corona, and that the efficiency of the process is probably related to the local magnetic topology, being more efficient in less divergent magnetic field lines.

UVCS is a joint project of the National Aeronautics and Space Administration (NASA), the Agenzia Spaziale Italiana (ASI), and the Swiss Founding Agencies. The authors wish to acknowledge the support of ASI, through contract ASI/I/035/05/0, and of the Ministero dell'Istruzione, dell'Università e della Ricerca (MIUR) and the Istituto Nazionale di Astrofisica (INAF), through grant COFIN-2003.

REFERENCES

Abbo, L., & Antonucci, E. 2002, in Proceedings of the Second Solar Cycle and Space Weather Euroconference, ed. H. Sawaya-Lacoste (ESA SP-477; Noordwijk: ESA), 323
Antonucci, E., Abbo, L., & Dodero, M. A. 2005, A&A, 435, 699
Antonucci, E., Dodero, M. A., & Giordano, S. 2000, Sol. Phys., 197, 115
Antonucci, E., Dodero, M. A., Giordano, S., Krishnakumar, V., & Noci, G. 2004, A&A, 416, 749
Antonucci, E., & Giordano, S. 2001, in Solar and Galactic Composition, ed. R. F. Wimmer-Schweingruber (Melville: AIP), 77
Antonucci, E., et al. 1997, in ASP Conf. Ser. 118, 1st Advances in Solar Physics Euroconference: Advances in Physics of Sunspots, ed. B. Schmieder, J. C. del Toro Iniesta, & M. Vazquez (San Francisco: ASP), 273
Arnaud, M., & Rothenflug, R. 1985, A&AS, 60, 425
Asplund, M., Grevesse, N., Sauval, A. J., Allende Prieto, C., & Kiselman, D. 2004, A&A, 417, 751
Cranmer, S. R., et al. 1999, ApJ, 511, 481
Curdt, W., Brekke, P., Feldman, U., Wilhelm, K., Dwivedi, B. N., Schühle, U., & Lemaire, P. 2001, A&A, 375, 591
David, C., et al. 1998, A&A, 336, L90
Frazin, R. A., Cranmer, S. R., & Kohl, J. L. 2003, ApJ, 597, 1145
Gibson, S. E., et al. 1999, J. Geophys. Res., 104, 9691
Grevesse, N., & Sauval, A. J. 1998, Space Sci. Rev., 85, 161
Guhathakurta, M., et al. 1999, J. Geophys. Res., 104, 9801
Kohl, J. L., et al. 1997, Sol. Phys., 175, 613
Marocchi, D., Antonucci, E., & Giordano, S. 2001, Ann. Geophys., 19, 135
Mazzotta, P., Mazzitelli, G., Colafrancesco, S., & Vittorio, N. 1998, A&AS, 133, 403
Noci, G., et al. 1997, in Fifth *SOHO* Workshop: The Corona and Solar Wind Near Minimum Activity, ed. A. Wilson (ESA SP-404; Noordwijk: ESA), 75
Raymond, J. C., Suleiman, R., van Ballegooijen, A., & Kohl, J. L. 1997a, in Correlated Phenomena at the Sun, in the Heliosphere and in Geospace, ed. A. Wilson (ESA SP-415; Noordwijk: ESA), 383
Raymond, J. C., et al. 1997b, Sol. Phys., 175, 645
Spitzer, L. 1962, Physics of Fully Ionized Gases (2nd ed.; New York: Interscience)
Strachan, L., et al. 2002, ApJ, 571, 1008
Verner, D. A., & Ferland, G. J. 1996, ApJS, 103, 467
von Steiger, R., Wimmer-Schweingruber, R. F., Geiss, J., & Gloeckler, G. 1995, Adv. Space Res., 15(7), 3
von Steiger, R., et al. 2000, J. Geophys. Res., 105, 27217
Vornov, G. S. 1997, At. Data Nucl. Data Tables, 65, 1
Wang, Y. H., & Sheeley, N. R. 1990, ApJ, 355, 726
Withbroe, G. L., et al. 1982, Space Sci. Rev., 33, 17